

# A mitochondrial disease model is generated and corrected using engineered base editors in rat zygotes

Received: 23 January 2025

Accepted: 24 April 2025

Published online: 03 June 2025

 Check for updates

Liang Chen<sup>1,2,9</sup>✉, Changming Luan<sup>3,9</sup>, Mengjia Hong<sup>3,9</sup>, Meng Yuan<sup>3</sup>, Hao Huang<sup>3</sup>, Debo Gao<sup>4</sup>, Xinyuan Guo<sup>3</sup>, Zhengxin Chen<sup>1</sup>, Yongmei Li<sup>3</sup>, Lei Yang<sup>3</sup>, Zongyi Yi<sup>5</sup>, Wensheng Wei<sup>5,6</sup>, Mingyao Liu<sup>7</sup>, Liangcai Gao<sup>3</sup>, Honghui Han<sup>3</sup> & Dali Li<sup>2,3,8</sup>✉

Efficient generation and correction of mutations in mitochondrial DNA (mtDNA) is challenging. Here, through embryonic injection of an mtDNA adenine base editor (eTd-mtABE), Leigh syndrome rat models were generated efficiently (up to 74%) in the F<sub>0</sub> generation, exhibiting severe defects. To correct this mutation, a precise mtDNA C-to-T base editor was engineered and injected into mutated embryos. It achieved restoration of wild-type alleles to an average of 53%, leading to amelioration of disease symptoms.

Point mutations are responsible for 95% of mitochondrial DNA (mtDNA) pathogenic mutations<sup>1</sup>, yet efficiently generating targeted point mutations in mtDNA to model or correct the disease remains challenging. Although a proven method exists for creating trans-mitochondrial cytoplasmic hybrid cells (cybrids) to model mtDNA diseases in cells and mice<sup>2</sup>, the technical complexity and lack of tools for introducing specific mtDNA mutations hinder the efficient generation of mtDNA disease models, which are essential for elucidating pathogenic mechanisms and advancing therapeutic development<sup>3,4</sup>. Unlike nuclear DNA mutation-induced genetic disorder, mtDNA diseases currently have no curative therapies<sup>3</sup>. As mitochondrial replacement therapy is the only intervention to prevent the transmission of mutant mtDNA between generations, there is an urgent demand for the development and demonstration of technology to directly correct the pathogenic mtDNA mutations without introducing nonparental DNA.

mtDNA base-editing technologies, enabling C-to-T or A-to-G base conversions, are very promising for disease modeling and potentially for intervention of mtDNA diseases through direct correction of pathogenic mutations. Mitochondrial cytosine base editors (DdCBEs),

comprising transcription activator-like effector (TALE) arrays, mitochondrial targeting sequences (MTSs), cytosine deaminase DddAtox and a uracil glycosylase inhibitor (UGI), enable C•G-to-T•A conversions in mtDNA<sup>5,6</sup>. Recently, through substitution of UGI to TadA-8e adenosine deaminase in DdCBE backbones, mtDNA adenine base editors (ABEs) named TALE-linked deaminases (TALEDs) were developed for targeted A•T-to-G•C mutation in mtDNA. However, compared to TadA-derived CRISPR-based nuclear ABEs, TALEDs catalyzed limited editing efficiency (especially A-to-G mutations) in animals. This aggravates the unavailability of mtDNA disease animal models whose phenotypes rely heavily on high levels of mtDNA mutations above a threshold (typically >50%)<sup>7–10</sup>. As rapid and efficient modeling in animals using canonical mitochondrial A-to-G editors remains challenging<sup>9</sup>, a recent study engineered strand-selective mitochondrial base editors encoded by circular RNA, which enabled robust mtDNA adenine base editing in mouse zygotes<sup>11</sup>. We applied efficient eTd-mtABE variants reported in our companion study<sup>12</sup> to generate a heritable rat mtDNA disease model. A pathogenic mtDNA single-nucleotide variant (m.14487T>C mutation in the *ND6* gene) causing Leigh syndrome<sup>13,14</sup> was selected for targeting (Fig. 1a,b).

<sup>1</sup>Lingang Laboratory, Shanghai, China. <sup>2</sup>School of Pharmacy, East China Normal University, Shanghai, China. <sup>3</sup>Shanghai Frontiers Science Center of Genome Editing and Cell Therapy, Shanghai Key Laboratory of Regulatory Biology, Institute of Biomedical Sciences and School of Life Sciences, East China Normal University, Shanghai, China. <sup>4</sup>School of Pharmacy, East China University of Science and Technology, Shanghai, China. <sup>5</sup>Biomedical Pioneering Innovation Center, Peking-Tsinghua Center for Life Sciences, Peking University Genome Editing Research Center, State Key Laboratory of Protein and Plant Gene Research, School of Life Sciences, Peking University, Beijing, China. <sup>6</sup>Changping Laboratory, Beijing, China. <sup>7</sup>BRL Medicine, Inc., Shanghai, China. <sup>8</sup>Shanghai Academy of Natural Sciences (SANS), Shanghai, China. <sup>9</sup>These authors contributed equally: Liang Chen, Changming Luan, Mengjia Hong. ✉e-mail: [chenliang@lglab.ac.cn](mailto:chenliang@lglab.ac.cn); [dlli@bio.ecnu.edu.cn](mailto:dlli@bio.ecnu.edu.cn)

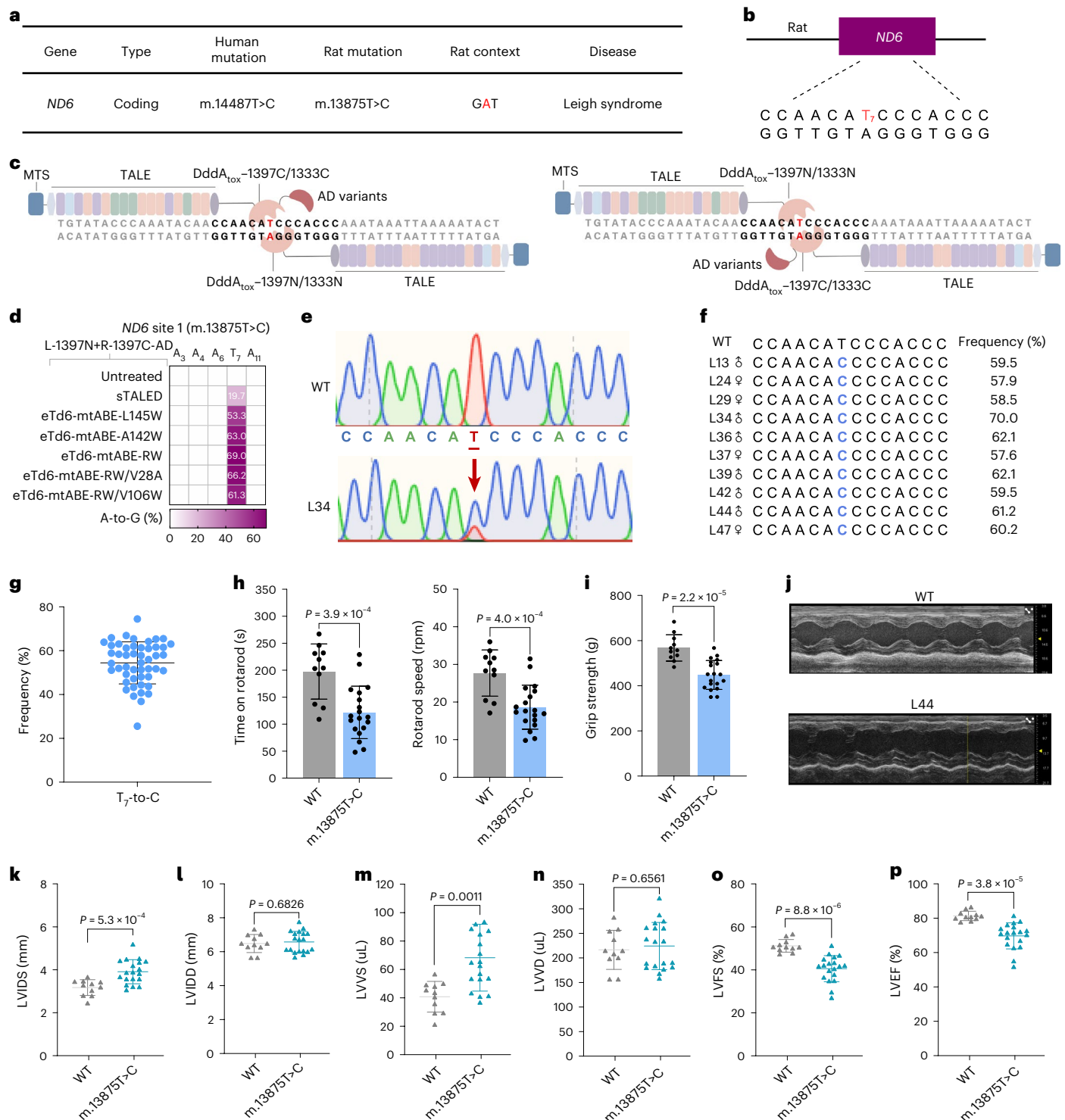


**Fig. 1 | Mitochondrial disease models generated by eTd-mtABEs in rats.**

**a**, Leigh syndrome-associated mutations in human mtDNA and corresponding rat mtDNA. Pathogenic mutation sites are highlighted in red. **b**, The target sequence of the rat mitochondrial ND6 gene is shown. The pathogenic position is shown in red. **c**, Architecture of eTd-mtABEs to target ND6 site 1. **d**, Heat map showing frequencies of mitochondrial A-to-G conversion treated with indicated editors targeting the ND6 site 1 in PC12 cells. Data represent the mean of three biologically independent replicates. **e**, Sanger sequencing chromatogram of ND6 site 1 in a wild-type (WT) rat and a representative F<sub>0</sub> founder. The red arrow indicates the target site. **f**, Genotyping of representative F<sub>0</sub> founders. The desired T<sub>7</sub>-to-C conversion is highlighted in blue. Frequencies of mutant alleles were determined by HTS. **g**, Desired T<sub>7</sub>-to-C editing frequencies of F<sub>0</sub>

founders with m.13875T>C mutation ( $n = 49$ ). **h**, Motor coordination of WT rats ( $n = 11$ ) and F<sub>0</sub> founders ( $n = 19$ ) at 11 weeks old was evaluated by a rotating rod test, with time on rotarods (left) and rotarod speed (right). **i**, Grip strength of mutant F<sub>0</sub> rats with m.13875T>C ( $n = 19$ ) was measured by grip strength test compared to WT rats ( $n = 11$ ) at 11 weeks old. **j**, Snapshots of M-mode of echocardiographic measurements including a WT rat and a representative rat. **k–p**, Echocardiographic measurements of WT rats ( $n = 11$ ) and F<sub>0</sub> founders ( $n = 19$ ) at 12 weeks old. Tests include LVIDS (**k**), LVIDD (**l**), LVVS (**m**), LVVD (**n**), LVFS (**o**) and LVEF (**p**). In **g–i** and **k–p**, data represent the mean  $\pm$  s.d. and each data point represents an individual rat. For **h, i** and **k–p**,  $P$  values were calculated using an unpaired Student's  $t$ -test (two-tailed).

In previous work<sup>12</sup>, we generated highly efficient eTd-mtABE variants (bearing A142W, L145W and A142R/L145W, denoted as RW, RW/V28A and RW/V106W, respectively). To screen the optimal eTd-mtABE construct for targeting *ND6* site 1 to model Leigh syndrome, we tested 40 eTd-mtABE constructs containing distinct TadA mutations fused to either left (L-AD) or right (R-AD) TALE arrays with different split orientations of DddAtox, targeting T<sub>7</sub> of mitochondrial *ND6* site 1 to induce an m.13875 (corresponding to human m.14487) T-to-C mutation in PC12 cells (Fig. 1c,d and Supplementary Fig. 1a–d). In the R-AD version, all eTd6-mtABEs achieved high mutation rates (40–69%) of nearly single-base T<sub>7</sub>-to-C editing compared to sTALED, which only induced 7.5–20% editing (Fig. 1d and Supplementary Fig. 1b,d). Then, the eTd6-mtABE-RW/V28A construct was selected and injected into rat zygotes, as we showed that introduction of V28A dramatically reduced DNA and RNA off-target effects in cells<sup>12</sup>. High-throughput sequencing (HTS) data revealed robust desired editing in all 49 F<sub>0</sub> rats with efficiency ranging from 26% to 74% (54% on average). Minimal bystander mutations (T<sub>4</sub>, averaging 2%) in the TALE-binding region were observed in founders (Fig. 1e–g and Supplementary Fig. 2a). Analysis of the editing outcomes in different organs showed similar mitochondrial adenine conversion ratios across various organs in each founder (Supplementary Fig. 2b). These on-target mtDNA mutations were efficiently transmitted to the F<sub>1</sub> and F<sub>2</sub> generations with the ratio increasing to 98.5%, while the bystander mutation (T<sub>4</sub>) in the TALE-binding region was further reduced to a minimal level (averaging 0.9% in F<sub>1</sub> pups and 0.02% in F<sub>2</sub> pups) after two generations of breeding (Fig. 1g and Supplementary Fig. 2c–g).

As Leigh syndrome in human is associated with skeletal muscle and heart defects<sup>14,15</sup>, we leveraged the rotarod test and grip strength test to assess the founder rats. The results indicated dramatic impairments in motor coordination, body balance and forelimb grip strength in the founders (Fig. 1h,i and Supplementary Fig. 3a,b). Furthermore, echocardiography confirmed abnormal cardiac structure and function, including dilated heart chambers, increased left-ventricular volume at end of systole (LVVS) and decreased left-ventricular ejection fraction (LVEF) (Fig. 1j–p and Supplementary Fig. 3c–h), suggesting successful generation of a mitochondrial disease model of Leigh syndrome. We observed gender-biased phenotypic manifestations of the disorder; female founders were more susceptible to muscle defects, whereas cardiac abnormalities were more prominent in male founders (Supplementary Fig. 3c–h). These data demonstrate that the eTd-mtABE variant is highly efficient for generating heritable mtDNA disease models in rats exhibiting apparent defects.

Previous studies showed that a heteroplasmy shift toward wild-type mtDNA is achievable through mitochondrially targeted site-specific nucleases to cleave and eliminate mutant mtDNA<sup>16</sup>. However, heteroplasmy shifting approaches using programmable nucleases rely on wild-type mitochondrial fission after elimination of mutant mtDNA, which is impractical for treating near-homoplasmic mtDNA mutations, such as establishment of Leigh syndrome rats from an F<sub>2</sub> generation bearing 99% T<sub>7</sub>-to-C mutations (Fig. 2a). We aimed to explore the feasibility of correcting the pathogenic point mutation through mtDNA cytosine base editing. Given that the target cytosine (C<sub>7</sub>) is located in an unfavorable AC motif for DdCBE<sup>5,17</sup> within a homopolymeric cytosine target site (Fig. 2b), it was challenging to correct the mutation with both high efficiency and accuracy. Base conversions of C<sub>5</sub> to T and C<sub>8</sub> to T were synonymous mutations but we still needed to engineer a DdCBE variant with a narrow editing window to minimize undesired bystander edits causing missense mutations (Fig. 2b and Supplementary Fig. 4a).

DdCBEs incorporating evolved DddA6/I1 deaminases<sup>17</sup>, which exhibited high activity with expanded sequence context preference, were selected for further engineering. Four additional mutations known to enhance mtDNA-editing specificity were individually introduced into the DddA6 or DddA11 variant<sup>18,19</sup>. These ten DddA variants

were then fused with two sets of TALE arrays (featuring short or long spacers) to create a total of 60 new DdCBE variants, arranged under either G1397-split or G1333-split orientation (Supplementary Fig. 4b,c). These DdCBE variants were tested in homoplasmic fibroblasts (99.9% of T<sub>7</sub>-to-C mutation) derived from newborn F<sub>2</sub> Leigh syndrome rats. HTS data showed that DdCBE variants with a short spacer (targeting *ND6* site 3) generally induced much higher activity with a slightly narrower editing window compared to the variants with a long spacer (targeting *ND6* site 2) in primary fibroblasts of Leigh syndrome rats (Fig. 2c and Supplementary Fig. 4d,e). Among them, the 1397NC-DddA11-V1411A variant induced the highest C<sub>7</sub>-to-T correction (up to 55%) with a relatively condensed editing window (positions 7–9) but also induced considerable undesired bystander C<sub>9</sub>-to-T edits (Fig. 2d,e). The 1333NC-DddA11-K1389A variant dramatically reduced the bystander edits, leaving a 2-nt (C<sub>7</sub>-C<sub>8</sub>) editing window (Fig. 2c), which led to 25% desired functional alleles containing C<sub>7</sub>-to-T correction regardless of synonymous mutations (Fig. 2e).

Next, we attempted to use the high-precision variant 1333NC-DddA11-K1389A to directly correct point mutation Leigh syndrome rats (Fig. 2f). Zygotes from nearly homoplasmic female rats (averaging 91.3% T<sub>7</sub>-to-C mutation) were collected and injected with mRNA encoding the aforementioned DdCBE variant. A total of 12 live pups were obtained, exhibiting highly efficient and precise correction of the m.13875T>C mutation (averaging 53% efficiency, ranging from 44% to 59%) with minimal bystander edits (averaging 10% in C<sub>9</sub> and 0.3% in C<sub>10</sub>). Among them, seven pups carried efficiently corrected m.13875T>C mutations with frequencies of over 50% (Fig. 2g,h and Supplementary Fig. 5a–d). Consistent with the editing outcomes observed in primary cells, the engineered DdCBE variant demonstrated highly efficient on-target C<sub>7</sub> editing within a narrow editing window in F<sub>0</sub> founders (Fig. 2c and Supplementary Fig. 5c,d). An average of 42% alleles contained the desired C<sub>7</sub>-to-T correction without missense mutation in all pups (Fig. 2i), further confirming the accuracy of 1333NC-DddA11-K1389A *in vivo*. Additionally, correction of the m.13875T>C mutation was consistently maintained throughout the pups' development (Supplementary Fig. 5e).

To investigate whether the ratio of C-to-T correction could ameliorate Leigh syndrome, phenotypic evaluations were performed. The rotarod test and grip strength test revealed that the near-homoplasmic (94% on average) F<sub>3</sub> rats showed severe defects in motor coordination, body balance and forelimb grip strength compared to wild-type controls (Fig. 2j,k and Supplementary Fig. 5f–j), which was consistent with the observation in F<sub>0</sub> founders (Fig. 1h,i), despite the fact that testing was conducted at different ages. Rats derived from Leigh syndrome embryos that were edited with 1333NC-DddA11-K1389A exhibited similar levels of muscle function to wild-type controls and demonstrated substantial improvement compared to homoplasmic m.13875T>C rats (Fig. 2j,k and Supplementary Fig. 5g–j). A more beneficial muscle recovery in female rats were observed (Supplementary Fig. 5g–j). Then, six representative edited rats were selected to investigate their heart function. Echocardiography experiments revealed apparent correction of cardiac abnormalities in the edited rats, with the observed parameters being similar to those of wild-type controls (Fig. 2l–n and Supplementary Fig. 5k–u). The correction efficiency is theoretically correlated with phenotypic alleviation. However, this correlation was not observed in DdCBE-injected Leigh syndrome rats, as varying correction rates resulted in similar levels of phenotypic improvement (Supplementary Fig. 5v–x). This lack of correlation may be attributed to the high correction efficiency (44–59%) achieved by the engineered DdCBE, which is likely below the threshold required to induce severe symptoms in this model. Because it was reported that incorporating the K1389A substitution into the split-dimer interface of DddAtox significantly reduced mitochondrial genome-wide off-target activity of DdCBEs<sup>18</sup>, we also found that the editing window of the 1333NC-DddA11-K1389A variant was narrower than other highly active DdCBEs. This suggests

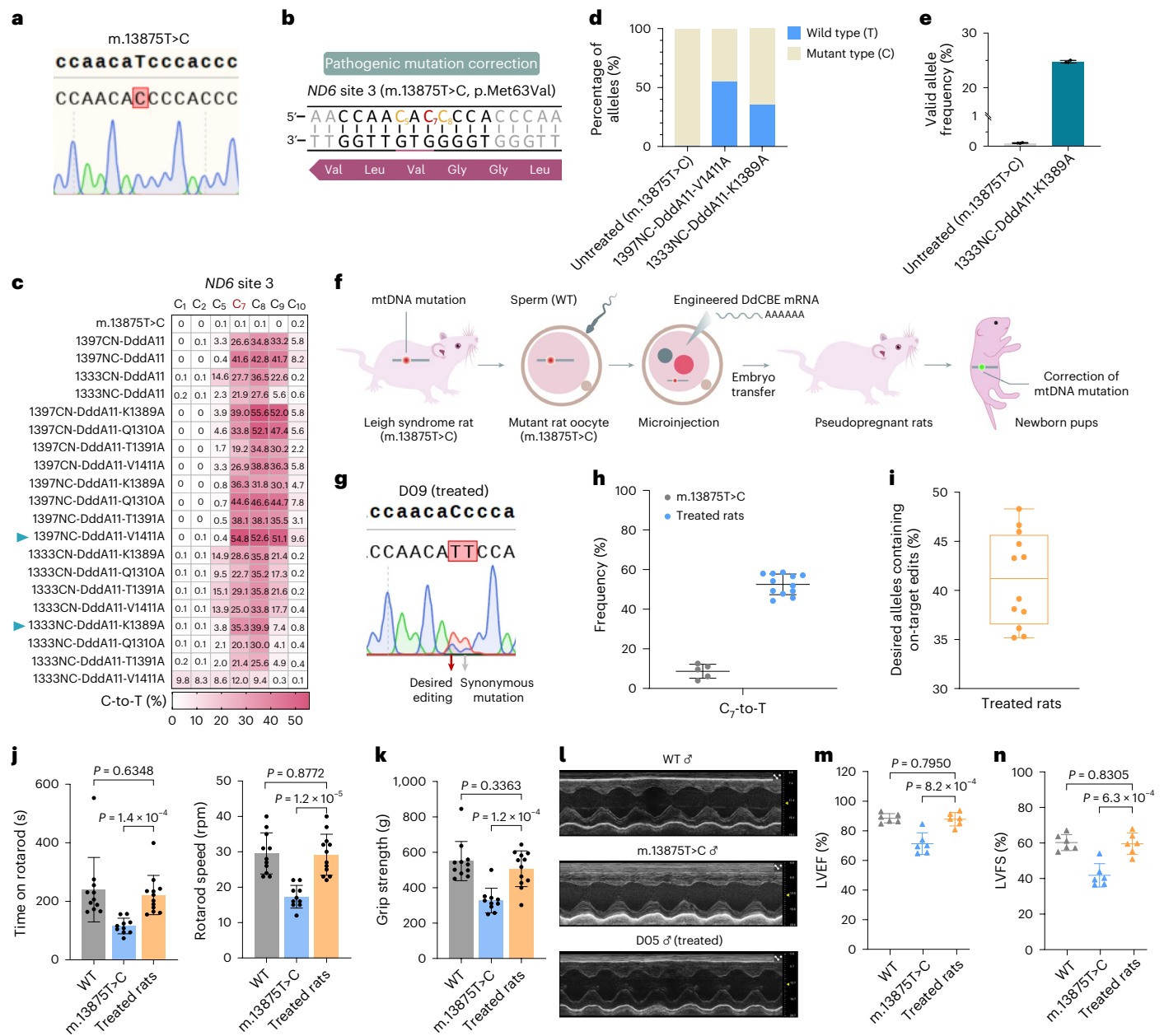


**Fig. 2 | Therapeutic editing of Leigh syndrome rats with engineered DdCBEs.** **a**, Sanger sequencing chromatogram of ND6 site 1 in the representative F<sub>2</sub> pup-derived fibroblasts with m.13875T>C. **b**, Diagram of the target site of the pathogenic mutation (ND6 site 3, m.13875T>C) in Leigh syndrome rat cells to be corrected by DdCBE. The red letter indicates the target mutation and yellow letters indicate synonymous mutations. **c**, Heat map showing the editing efficiency of indicated editors targeted to ND6 site 3 in primary cells. **d**, The percentage of mutant (C) and WT (T) alleles at position 7 of the spacer in untreated primary cells and cells treated with indicated editors with the data from **c**. **e**, The valid allele frequencies in untreated or DdCBE variant treated primary cells. Data are the mean ± s.d. of n = 3 independent replicates. **f**, The workflow for DdCBE-mediated correction of Leigh syndrome mutation in rats. **g**, Sanger sequencing chromatogram of DNA from representative F<sub>0</sub> rat (D09) injected with engineered DdCBE mRNA. **h**, C<sub>7</sub>-to-T editing frequencies of untreated (m.13875T>C; n = 5) and treated (n = 12) rats with indicated editors. **i**, Efficiency of desired corrected alleles containing on-target C<sub>7</sub>-to-T edits in treated rats (n = 12). In the box plot, the

box spans the interquartile range (first to third quartile) and the horizontal line indicates the median (second quartile). The lower and upper whiskers indicate the minimum and maximum values within 1.5 times the interquartile range from the first and third quartiles, respectively. Data points in the plot represent the full range of values plotted. Each single dot represents an individual rat. **j**, Motor coordination of WT (n = 11), m.13875T>C (n = 10) and treated rats (n = 12) at 8 weeks old was evaluated by a rotating rod test, with time on rotarods (left) and rotarod speed (right). **k**, Grip strength measured by grip strength test of treated (n = 12), WT (n = 11) and m.13875T>C (n = 10) rats at 8 weeks old. **l**, Snapshots of M-mode of echocardiographic measurements including representative WT, m.13875T>C and treated rats at 9 weeks old. **m, n**, Echocardiographic measurements including LVEF (**m**) and LVFS (**n**) of WT (n = 6), m.13875T>C (n = 6) and treated (n = 6) rats at 9 weeks old. In **c, d**, data represent the mean of three biologically independent replicates. In **h–k, m, n**, data represent the mean ± s.d. and each data point represents an individual rat. In **j, k, m, n**, P values were calculated using an unpaired Student's *t*-test (two-tailed).

that editing the m.13875T>C site using the 1333NC-DddA11-K1389A variant would not induce considerable off-target editing across the entire mtDNA in this rat model. However, experimental validation of

potential genomic DNA off-target effects remains essential for future therapeutic applications. Taken together, these results suggest that our accurate DdCBE variant is highly efficient in zygotes for correcting

pathogenic mtDNA mutations and ameliorating the Leigh syndrome phenotype in rats, thereby encouraging the development of new treatments for mtDNA diseases through the correction of point mutations.

mtDNA diseases are currently incurable and cause substantial illness and premature death<sup>7</sup>. In this study, we demonstrated that evolved hyperactive eTd-mtABE-RW/V28A exhibited high specificity in installing pathogenic mutations in rat embryos and achieved a very high point mutation rate to model Leigh syndrome. We further demonstrated that the eTd-mtABE variant is a superb editor with high efficiency and accuracy. This rapid and efficient modeling methodology, reliant on advanced mitochondrial ABEs, substantially enhances the ability to investigate mtDNA-related diseases, offering a powerful tool for advancing research in this critical field. Therapeutic intervention for mitochondrial diseases is usually very challenging and, to our knowledge, no study has been reported on the direct correction of mtDNA mutations in animal models. Through engineering and screening of 60 DdCBE variants, we obtained a new DdCBE variant with a condensed editing window and high efficiency for correcting the pathogenic m.13875T>C mutation in rat zygotes, substantially reduced the transmission of mtDNA mutation and ameliorated Leigh syndrome phenotypes in rats. To date, the only practical method for intervening in mtDNA diseases is mitochondrial replacement therapy, which may risk the inadvertent transfer of perinuclear mtDNA into the recipient oocyte or zygote, thereby raising ethical concerns<sup>20</sup>. Although mtDNA base editing is still in its infancy and there will be a long journey to improve it before clinical applications can be realized, our study demonstrates a method for potentially treating mtDNA diseases. This could represent a favorable alternative to mitochondrial replacement therapy and programmable nuclease-mediated heteroplasmy shifting in various cases.

### Online content

Any methods, additional references, Nature Portfolio reporting summaries, source data, extended data, supplementary information, acknowledgements, peer review information; details of author contributions and competing interests; and statements of data and code availability are available at <https://doi.org/10.1038/s41587-025-02684-y>.

### References

- Kim, J. S. & Chen, J. Base editing of organellar DNA with programmable deaminases. *Nat. Rev. Mol. Cell Biol.* **25**, 34–45 (2024).
- Stewart, J. B. Current progress with mammalian models of mitochondrial DNA disease. *J. Inherit. Metab. Dis.* **44**, 325–342 (2021).
- Silva-Pinheiro, P. & Minczuk, M. The potential of mitochondrial genome engineering. *Nat. Rev. Genet.* **23**, 199–214 (2022).
- Russell, O. M., Gorman, G. S., Lightowlers, R. N. & Turnbull, D. M. Mitochondrial diseases: hope for the future. *Cell* **181**, 168–188 (2020).
- Mok, B. Y. et al. A bacterial cytidine deaminase toxin enables CRISPR-free mitochondrial base editing. *Nature* **583**, 631–637 (2020).
- Cho, S. I. et al. Targeted A-to-G base editing in human mitochondrial DNA with programmable deaminases. *Cell* **185**, 1764–1776 (2022).
- Gorman, G. S. et al. Mitochondrial diseases. *Nat. Rev. Dis. Primers* **2**, 16080 (2016).
- Patananan, A. N., Wu, T. H., Chiou, P. Y. & Teitell, M. A. Modifying the mitochondrial genome. *Cell Metab.* **23**, 785–796 (2016).
- Cho, S. I. et al. Engineering TALE-linked deaminases to facilitate precision adenine base editing in mitochondrial DNA. *Cell* **187**, 95–109 (2024).
- Chen, L. et al. Engineering a precise adenine base editor with minimal bystander editing. *Nat. Chem. Biol.* **19**, 101–110 (2023).
- Zhang, X. et al. Precise modelling of mitochondrial diseases using optimized mitoBEs. *Nature* **639**, 735–745 (2025).
- Chen, L. et al. Efficient mitochondrial A-to-G base editors for the generation of mitochondrial disease models. *Nat. Biotechnol.* <https://doi.org/10.1038/s41587-025-02685-x> (2025).
- Khoo, A. et al. Progressive myoclonic epilepsy due to rare mitochondrial ND6 mutation, m.14487T>C. *BMJ Neurol. Open* **3**, e000180 (2021).
- Thorburn, D. R., Rahman, J. & Rahman, S. Mitochondrial DNA-associated Leigh syndrome and NARP. In *GeneReviews* (eds Adam, M. P. et al.) (University of Washington, 1993).
- Dermaut, B. et al. Progressive myoclonic epilepsy as an adult-onset manifestation of Leigh syndrome due to m.14487T>C. *J. Neurol. Neurosurg. Psychiatry* **81**, 90–93 (2010).
- Lim, K. Mitochondrial genome editing: strategies, challenges, and applications. *BMB Rep.* **57**, 19–29 (2024).
- Mok, B. Y. et al. CRISPR-free base editors with enhanced activity and expanded targeting scope in mitochondrial and nuclear DNA. *Nat. Biotechnol.* **40**, 1378–1387 (2022).
- Lee, S., Lee, H., Baek, G. & Kim, J. S. Precision mitochondrial DNA editing with high-fidelity DddA-derived base editors. *Nat. Biotechnol.* **41**, 378–386 (2023).
- Lei, Z. et al. Mitochondrial base editor induces substantial nuclear off-target mutations. *Nature* **606**, 804–811 (2022).
- Adashi, E. Y., Rubenstein, D. S., Mossman, J. A., Schon, E. A. & Cohen, I. G. Mitochondrial disease: replace or edit? *Science* **373**, 1200–1201 (2021).

**Publisher's note** Springer Nature remains neutral with regard to jurisdictional claims in published maps and institutional affiliations.

Springer Nature or its licensor (e.g. a society or other partner) holds exclusive rights to this article under a publishing agreement with the author(s) or other rightsholder(s); author self-archiving of the accepted manuscript version of this article is solely governed by the terms of such publishing agreement and applicable law.

© The Author(s), under exclusive licence to Springer Nature America, Inc. 2025

## Methods

### Plasmid construction

The primers used in this study are listed in Supplementary Table 1. Amino acid and nucleotide sequences are listed in Supplementary Table 3. The primers and oligonucleotides were synthesized by Biosune. TALED\_Left-ND1-1397C-AD (183892), TALED\_Right-ND1-1397N (183898), ND4.2-Left TALE-G1397-N-DddA11-mCherry (179682) and ND4.2-Right DdCBE-G1397-C-T14131-GFP (179686) plasmids were purchased from Addgene. New mitochondrial base editor plasmids were constructed using previously published methods<sup>21,22</sup>. In brief, DNA fragments were amplified using PrimeSTAR Max DNA polymerase (Takara) and assembled with a 2× MultiF seamless assembly mix (Abclonal) according to the manufacturer's protocol. The TALE arrays targeting disease-associated mutations in rat mtDNA were constructed using Golden Gate (New England Biolabs). All TALE array sequences are listed in Supplementary Table 2. eTd-mtABEs were replaced by TadA-8e and DddAtox variants based on sTALEDs. Engineered DdCBEs were constructed by site-directed mutagenesis using a PCR-based method based on original editors. For flow cytometry assay, double-strand mtDNA-editing constructs were modified with mCherry or GFP using a P2A sequence. Plasmids were transformed into DH5α chemically competent cells (TransGen Biotech). Plasmids used for transfection were isolated using the Tiangen plasmid mini extraction kit according to the manufacturer's instructions.

### Cell culture and transfection

Rat PC12 cells (American Type Culture Collection, CRL-1721) and primary rat m.13875T>C cells were cultured in DMEM (Gibco) supplemented with 10% (v/v) FBS (Gibco) and 1% (v/v) penicillin and streptomycin. All cell types were maintained at 37 °C with 5% CO<sub>2</sub>. PC12 cells and primary rat m.13875T>C cells were passaged every 3 or 4 days. For evaluating the mitochondrial base editing, PC12 cells and primary rat m.13875T>C cells were seeded in 12-well plates (Corning) and transfected with 1,600 ng of each eTd-mtABE, sTALED or DdCBE variant monomer at 70–80% confluence using Lipofectamine LTX (Thermo Fisher Scientific).

### Genomic DNA extraction and amplification

PC12 cells or primary rat m.13875T>C cells transfected after 72 h were washed with 1× PBS and digested with 0.25% trypsin (Gibco) for fluorescence-activated cell sorting. EGFP and mCherry double-positive cells were harvested and the genomic DNA was extracted using Quick-Extract DNA extraction solution (Lucigen) according to the manufacturer's recommended protocol. The extraction solution was incubated at 65 °C for 6 min and then 98 °C for 2 min. To obtain the genotype of modified and treated rats, genomic DNA for PCR was extracted from collected tissues using traditional isopropyl method. Genome loci of interest were amplified with site-specific primers listed in Supplementary Table 1 using KOD-Plus-Neo DNA Polymerase (Toyobo).

### mRNA preparation

In vitro transcription (IVT) template DNAs were prepared by linearizing with EcoRI and extracted using the phenol–chloroform method. eTd-mtABE and engineered DdCBE mRNAs were synthesized using Hi-yield T7 IVT reagent (NI-Me-pUTP, Hzymes) according to the manufacturer's protocol. In brief, after 2-h incubation at 37 °C, 1 μl of DNase I was added into the solution and incubated at 37 °C for 15 min to digest the template DNA. Subsequently, IVT reaction solution was purified by ammonium acetate and washed with precooled 70% ethanol. mRNA was eluted in RNase-free water (Takara) and stored at –80 °C.

### Animals and microinjection of zygotes

Sprague–Dawley rats used in this study were purchased from Shanghai Jihui Textile Technology. Rats were maintained in specific-pathogen-free facilities at 20–22 °C with 40–60% humidity

under a 12-h light–dark cycle. All animal experiments met the regulations drafted by the Association for Assessment and Accreditation of Laboratory Animal Care in Shanghai and were approved by the Experimental Animal Welfare Ethics Committee of East China Normal University (ECNU; license number R20241214). Animal manipulations were in line with a previous report<sup>10</sup>. The mixture of eTd-mtABE-encoding or engineered DdCBE mRNAs (150 ng μl<sup>-1</sup> each) was diluted in RNase-free water and injected into the cytoplasm using an Eppendorf Transfer-Man NK2 micromanipulator. Injected zygotes were transferred into pseudopregnant female rats at 7–8 weeks old.

### Rotarod test

To assess the motor coordination of rats, a rotarod machine with automatic timers and falling sensor (XR-6D, Shanghai Xinruan Information Technology) was used. Rats were acclimated to the rotarod at a constant speed of 5 rpm for 10 min as training. The rotarod test was started at an initial speed of 4 rpm and accelerated uniformly to 40 rpm within 5 min. The time rats spent on the rotarod and the rotarod speed at which rats fell were recorded.

### Grip strength test

To evaluate the muscle strength of rats, the maximal force of the forelimbs was measured using a BIO-GS3 (Bioseb) according to the manufacturer's instructions. The rat hung on a metal bar with its forepaws until its grip failed while the tester pulled the tail of the rat. Three repeats were performed on each rat and the average data were calculated.

### Echocardiography analysis

The heart structure and function of mutant rats were evaluated by echocardiography. The m.13875T>C or treated rats were lightly anesthetized (heart rate ≥ 370 beats per min) and compared to same-aged wild-type rats. Echocardiographic observations were performed using a Vevo LAZR-X ultrasound machine with an MX250S probe (20 MHz). M-mode images were used to measure the internal diameter of the left ventricle measured at the end of systole (LVIDS) and diastole (LVIDD), LVVS, left-ventricular volume at end of diastole (LVVD), left-ventricular percentage fractional shortening (LVFS) and LVEF. Measurements were recorded at least three continuous cardiac cycles.

### Next-generation sequencing and data analysis

The second PCR amplifications were performed with primers containing an adaptor sequence (forward, 5'-GGAGTGAGTACGGTGTGC-3'; reverse, 5'-GAGTTGGATGCTGGATGG-3') and diverse barcode sequences at the 5' end. The resulting HTS libraries were pooled and purified by electrophoresis with a 1.5% agarose gel using HiPure gel pure DNA micro kit (Magen) eluting with 60 μl of H<sub>2</sub>O and then sequenced on an Illumina HiSeq platform. To assess base-editing efficiencies, A•T-to-G•C efficiencies and indels in the HTS data were analyzed using BE-Analyzer<sup>23</sup>. Base-editing efficiencies were calculated as the number of base substitution reads divided by total reads. Purities were calculated as the percentage of reads of A•T-to-G•C edits divided by reads of adenine edits without indels. Indel frequencies were calculated as the percentage of reads of indels divided by total reads.

### Statistical analysis and reproducibility

Data are presented as the mean ± s.d. from independent experiments. All statistical analyses were performed on *n* = 3 biologically independent experiments, unless otherwise noted in the figure captions, using GraphPad Prism version 9.3.1 software.

### Reporting summary

Further information on research design is available in the Nature Portfolio Reporting Summary linked to this article.

## Data availability

HTS data were deposited to the National Center for Biotechnology Information Sequence Read Archive database under accession code [PRJNA1252023](https://doi.org/10.1038/s41587-025-02684-y). There are no restrictions on data availability. Source data are provided with this paper.

## References

21. Chen, L. et al. Adenine transversion editors enable precise, efficient A•T-to-C•G base editing in mammalian cells and embryos. *Nat. Biotechnol.* **42**, 638–650 (2024).
22. Zhang, X. et al. Increasing the efficiency and targeting range of cytidine base editors through fusion of a single-stranded DNA-binding protein domain. *Nat. Cell Biol.* **22**, 740–750 (2020).
23. Hwang, G. H. et al. Web-based design and analysis tools for CRISPR base editing. *BMC Bioinformatics* **19**, 542 (2018).

## Acknowledgements

We thank Y. Zhang from the Flow Cytometry Core Facility of School of Life Sciences at ECNU and support from the ECNU Public Platform for innovation (O11). We thank L. Ji (HAVAS) for designing schematic diagrams. This work was partially supported by grants from the National Key R&D Program of China (2023YFC3403400 and 2023YFE0209200 to D.L.; 2024YFC3407900 to L.C.), National Natural Science Foundation of China (32025023, 32230064 and 32311530111 to D.L.; 31930016 to W.W.; 82230002 to M.L.), Innovation Program of Shanghai Municipal Education Commission (2019-01-07-00-05-E00054 to D.L.), Shanghai Municipal Commission for Science and Technology (24J22800400 to D.L.), Young Elite Scientist Sponsorship Program by China Association for Science and

Technology (2023QNRC001 to L.C.), Shanghai Oriental Talent Plan (QNZH2024131 to L.C.), Fellowship of China Postdoctoral Science Foundation (8206400139 to Z.Y.) and Lingang Laboratory. D.L. is a Shanghai Academy of Natural Sciences Exploration Scholar.

## Author contributions

L.C. and D.L. designed the experiments. L.C., C.L., M.H., M.Y., H. Huang, D.G., X.G., Y.L., L.Y., L.G. and H. Han performed the experiments. L.C., C.L., M.H., M.Y., H. Huang, D.G., X.G., Z.C., Z.Y., W.W., M.L. and D.L. analyzed the data. L.C. and D.L. wrote the paper with input from all authors. L.C. and D.L. supervised the research.

## Competing interests

The authors have submitted patent applications based on the results reported in this study (L.C., D.L., M.H. and C.L.). The other authors declare no competing interests.

## Additional information

**Supplementary information** The online version contains supplementary material available at <https://doi.org/10.1038/s41587-025-02684-y>.

**Correspondence and requests for materials** should be addressed to Liang Chen or Dali Li.

**Peer review information** *Nature Biotechnology* thanks the anonymous reviewers for their contribution to the peer review of this work.

**Reprints and permissions information** is available at [www.nature.com/reprints](http://www.nature.com/reprints).

## Reporting Summary

Nature Portfolio wishes to improve the reproducibility of the work that we publish. This form provides structure for consistency and transparency in reporting. For further information on Nature Portfolio policies, see our [Editorial Policies](#) and the [Editorial Policy Checklist](#).

### Statistics

For all statistical analyses, confirm that the following items are present in the figure legend, table legend, main text, or Methods section.

n/a Confirmed

- The exact sample size ( $n$ ) for each experimental group/condition, given as a discrete number and unit of measurement
- A statement on whether measurements were taken from distinct samples or whether the same sample was measured repeatedly
- The statistical test(s) used AND whether they are one- or two-sided  
*Only common tests should be described solely by name; describe more complex techniques in the Methods section.*
- A description of all covariates tested
- A description of any assumptions or corrections, such as tests of normality and adjustment for multiple comparisons
- A full description of the statistical parameters including central tendency (e.g. means) or other basic estimates (e.g. regression coefficient) AND variation (e.g. standard deviation) or associated estimates of uncertainty (e.g. confidence intervals)
- For null hypothesis testing, the test statistic (e.g.  $F$ ,  $t$ ,  $r$ ) with confidence intervals, effect sizes, degrees of freedom and  $P$  value noted  
*Give  $P$  values as exact values whenever suitable.*
- For Bayesian analysis, information on the choice of priors and Markov chain Monte Carlo settings
- For hierarchical and complex designs, identification of the appropriate level for tests and full reporting of outcomes
- Estimates of effect sizes (e.g. Cohen's  $d$ , Pearson's  $r$ ), indicating how they were calculated

*Our web collection on [statistics for biologists](#) contains articles on many of the points above.*

### Software and code

Policy information about [availability of computer code](#)

#### Data collection

Targeted amplicons sequencing data were collected and demultiplexed by an Illumina HiSeq XTen instrument. FACS gating data were collected on a FACSAria Fusion (BD Biosciences) using FACSDiva version 9.4 (BD Biosciences). Data of rotarod test and grip strength test were recorded using a rotarod machine (XR-6D) and BIO-GS3 (Bioseb). Data and image of echocardiographic measurements were collected using Vevo LAZR-X ultrasound machine.

#### Data analysis

High-throughput sequencing data were analyzed by BE-Analyzer (<http://www.rgenome.net/be-analyzer/#/>) (Hwang G-H et al, BMC Bioinformatics, 2018) or CRISPResso2 (<http://crispresso.pinellolab.partners.org/>) (Clement, K. et al. Nat Biotechnol, 2019) for base editing (A-T-to-G-C, and C-G-to-T-A) and indels efficiencies. FACS data was analyzed using FlowJo v.10. End-systole (LVIDS), end-diastole (LVIDD), left ventricular volume at end-systole and end-diastole (LVVS, LVVD), left ventricular percent fractional shortening (LVFS) and left ventricular ejection fraction (LVEF) were analyzed by VevoStrain software. GraphPad Prism 9.3.1 was also used to analyze data.

For manuscripts utilizing custom algorithms or software that are central to the research but not yet described in published literature, software must be made available to editors and reviewers. We strongly encourage code deposition in a community repository (e.g. GitHub). See the Nature Portfolio [guidelines for submitting code & software](#) for further information.

## Data

Policy information about [availability of data](#)

All manuscripts must include a [data availability statement](#). This statement should provide the following information, where applicable:

- Accession codes, unique identifiers, or web links for publicly available datasets
- A description of any restrictions on data availability
- For clinical datasets or third party data, please ensure that the statement adheres to our [policy](#)

Targeted amplicon sequencing data have been deposited in the NCBI Sequence Read Archive database under Accession Code PRJNA1252023.

## Research involving human participants, their data, or biological material

Policy information about studies with [human participants or human data](#). See also policy information about [sex, gender \(identity/presentation\), and sexual orientation](#) and [race, ethnicity and racism](#).

Reporting on sex and gender	N/A
Reporting on race, ethnicity, or other socially relevant groupings	N/A
Population characteristics	N/A
Recruitment	N/A
Ethics oversight	N/A

Note that full information on the approval of the study protocol must also be provided in the manuscript.

## Field-specific reporting

Please select the one below that is the best fit for your research. If you are not sure, read the appropriate sections before making your selection.

- Life sciences       Behavioural & social sciences       Ecological, evolutionary & environmental sciences

For a reference copy of the document with all sections, see [nature.com/documents/nr-reporting-summary-flat.pdf](https://www.nature.com/documents/nr-reporting-summary-flat.pdf)

## Life sciences study design

All studies must disclose on these points even when the disclosure is negative.

Sample size	Experiments were performed in biological triplicate n=3 unless otherwise noted. Sample sizes were opted to display the range and consistency of differences and three biological replicates made it sufficient to support the conclusions in this research. Sample sizes for these experiments were chosen based upon fields standards and prior knowledge of experimental variation.
Data exclusions	No data were excluded from the analysis.
Replication	Three independent biological replicates were performed on different days. All replications were successful.
Randomization	Samples were randomly distributed into groups.
Blinding	Investigators were not blinded to group allocation in this research since experimental conditions were evident and all samples of treatment were consistent throughout experiments.

## Reporting for specific materials, systems and methods

We require information from authors about some types of materials, experimental systems and methods used in many studies. Here, indicate whether each material, system or method listed is relevant to your study. If you are not sure if a list item applies to your research, read the appropriate section before selecting a response.

## Materials &amp; experimental systems

## Methods

- n/a  Involved in the study
- Antibodies
- Eukaryotic cell lines
- Palaeontology and archaeology
- Animals and other organisms
- Clinical data
- Dual use research of concern
- Plants

- n/a  Involved in the study
- ChIP-seq
- Flow cytometry
- MRI-based neuroimaging

## Eukaryotic cell lines

Policy information about [cell lines and Sex and Gender in Research](#)

- Cell line source(s)
- Authentication
- Mycoplasma contamination
- Commonly misidentified lines (See [ICLAC](#) register)

## Animals and other research organisms

Policy information about [studies involving animals; ARRIVE guidelines](#) recommended for reporting animal research, and [Sex and Gender in Research](#)

- Laboratory animals
- Wild animals
- Reporting on sex
- Field-collected samples
- Ethics oversight

Note that full information on the approval of the study protocol must also be provided in the manuscript.

## Plants

- Seed stocks
- Novel plant genotypes
- Authentication

## Plots

Confirm that:

- The axis labels state the marker and fluorochrome used (e.g. CD4-FITC).
- The axis scales are clearly visible. Include numbers along axes only for bottom left plot of group (a 'group' is an analysis of identical markers).
- All plots are contour plots with outliers or pseudocolor plots.
- A numerical value for number of cells or percentage (with statistics) is provided.

## Methodology

Sample preparation

Cell culture and transfection procedures are described in the methods. Cells were washed and filtered through a 45µm cell strainer cap before sorting (72h after transfection).

Instrument

FACSaria Fusion (BD Biosciences)

Software

FACSDiva version 9.4

Cell population abundance

The number of PC12 cells gated for target populations were similar in different biology replicates.

Gating strategy

For PC12 cells, gates were drawn to collect subsets of EGFP- and mCherry-double positive cells. Detailed gating strategy is provided in the Supplementary Note.

- Tick this box to confirm that a figure exemplifying the gating strategy is provided in the Supplementary Information.